

Review of Hadron Structure Calculations on a Lattice

Sergey Syritsyn*

RIKEN-BNL Research Center, Brookhaven National Laboratory, Upton, NY, 11973, USA

E-mail: syritsyn@alum.mit.edu

I present a review of the current status and the most recent achievements in lattice QCD calculations of hadron structure. First, I overview the status and systematic uncertainties of nucleon structure “benchmark” quantities that are well known from experiments and serve as a reference point for the validity of lattice QCD methods. Next, I discuss the current status of calculations of form factors of the nucleon and highlight some recent results for other hadrons that are important for understanding their internal dynamics. Wave functions of hadrons and their excitations may also be studied in lattice QCD, and I illustrate it with two recent examples of such calculations. Finally, I discuss in detail the state of calculations pertaining to the nucleon spin puzzle.

31st International Symposium on Lattice Field Theory - LATTICE 2013

July 29 - August 3, 2013

Mainz, Germany

*Speaker.

1. Benchmark quantities

With recent advances, the field of Lattice QCD is mature enough to provide reliable information about the world of nuclear physics. The first major breakthrough was a successful calculation of the hadron spectrum [1]. The next milestone that has nearly been reached is to verify that lattice QCD captures internal dynamics and structure of hadrons correctly. On this path, reproducing basic features about the most studied hadrons, the proton and the neutron, is an essential milestone. The nucleon structure observables discussed in this section have the least systematic ambiguity and stochastic error, and thus may be categorized as “lattice QCD benchmark” quantities.

1.1 Nucleon axial charge

The axial charge of the nucleon is an important quantity for the entire field of nuclear physics as it governs the rate of β -decay and, for instance, the neutron half-life, as a forward nucleon matrix element of the isovector axial-vector quark current,

$$\langle N(P) | \bar{q} \gamma^\mu \gamma^5 q | N(P) \rangle = g_A \bar{u}_P \gamma^\mu \gamma^5 u_P, \quad (1.1)$$

where u_P is the nucleon spinor, and which can be calculated without disconnected quark contractions ambiguity. Historically, most attempts to calculate this quantity resulted in values 10-15% below the experimental number, almost irrespective of the pion mass used. Until recently, it was easy to ascribe this discrepancy to heavy pion masses used. However, recent calculations with m_π approaching the physical point apparently continue this trend. Over the years, the deficiency has been ascribed to finite-volume effects (FVE) [2], excited state contributions [3, 4, 5] and finite-temperature effects [6]. There is no convincing evidence that any of these sources is solely responsible for the discrepancy; it is plausible that interplay of various systematic effects takes place, and with every collaboration using slightly different methods, meaningful comparisons are complicated. For instance, a better agreement was claimed upon removal of excited state contributions with a variational [3] and summation [4, 5] methods, while others [7, 8] did not detect significant excited state effects. The pattern of finite volume dependence, initially claimed in [2], was not confirmed when other collaboration results were examined [9]. Finite temperature dependence [6] was not confirmed in a subsequent detailed study [10] at $m_\pi \approx 250$ MeV (Fig. 2). Finally, there is a very encouraging agreement with experiment from the most recent study directly at the physical pion mass [11]. Hopefully, this preliminary result will be confirmed by other collaborations with careful evaluations of all systematic effects.

1.2 Quark momentum fraction

Another “benchmark” quantity is the isovector quark momentum fraction. It is measured in DIS experiments and, although its value depends on phenomenological models of parton distribution functions, different parameterizations yield agreeing results. Lattice calculation of this quantity involves the quark energy-momentum tensor operator,

$$\langle N(P) | \bar{q} \gamma_{\{\mu} \overleftrightarrow{D}_{\nu\}} q | N(P) \rangle = \langle x \rangle_q \bar{u}_P P_{\{\mu} \gamma_{\nu\}} u_P, \quad (1.2)$$

and typically is converted to $\overline{MS}(2 \text{ GeV})$ using the RI/MOM method [21]. Until recently, lattice results overwhelmingly overestimated the phenomenological value by 40 – 60%. Newer results

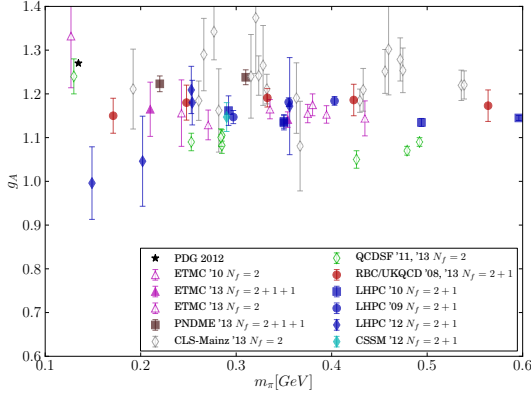


Figure 1: Summary of nucleon axial charge g_A lattice results [3, 12, 13, 9, 8, 4, 14, 15, 16, 17, 6].

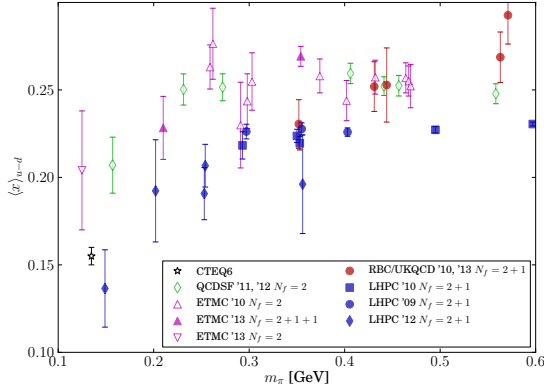


Figure 3: Summary of quark momentum fraction $\langle x \rangle_{u-d}^{MS(2 \text{ GeV})}$ lattice results [9, 18, 19, 20, 17, 6].

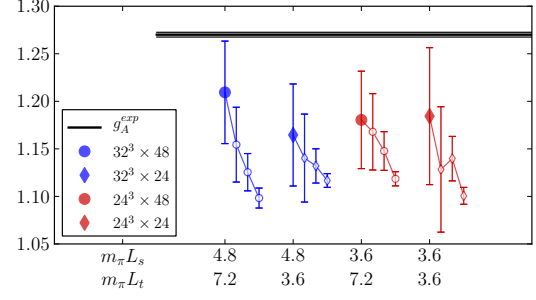


Figure 2: Detailed study of g_A dependence on volume and temperature with Wilson fermions, $m_\pi \approx 250 \text{ MeV}$ [10].

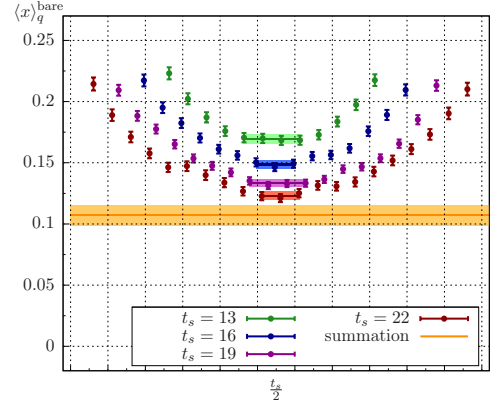


Figure 4: Excited state contributions to bare $\langle x \rangle_{u-d}$ and their removal using the summation method [5].

closer to the physical pion mass tend to approach the experimental value (Fig. 3). Such behavior is in agreement with corrections computed in Chiral Perturbation Theory (ChPT), $\delta^{\text{ChPT}} \langle x \rangle_{u-d} \sim m_\pi^2 \log m_\pi^2$, indicating that this quantity may change rapidly at lighter pion masses, thus precluding reliable chiral extrapolations. Many recent studies point out that this quantity suffers from substantial excited state effects [13, 5, 22], see Fig. 4, increasingly so towards the physical pion mass [6], where subtraction of excited state contributions has lead to agreement with experiment.

1.3 Nucleon radius and magnetic moment

Electromagnetic structure of the nucleon is characterized with the Dirac and Pauli form factors $F_{1,2}^q$:

$$\langle N(P+q) | \bar{q} \gamma^\mu q | N(P) \rangle = \bar{u}_{P+q} [F_1^q(Q^2) \gamma^\mu + F_2^q(Q^2) \frac{i \sigma^{\mu\nu} q_\nu}{2M_N}] u_P, \quad Q^2 = -q^2, \quad (1.3)$$

which will be discussed in more detail in Sect. 3.1. The small- Q^2 behavior of these form factors, $F^q(Q^2) = F(0) [1 + \frac{1}{6} Q^2 (r^2)^q + \mathcal{O}(Q^4)]$, is characterized by Dirac and Pauli $(r_{1,2}^2)^q$ radii of

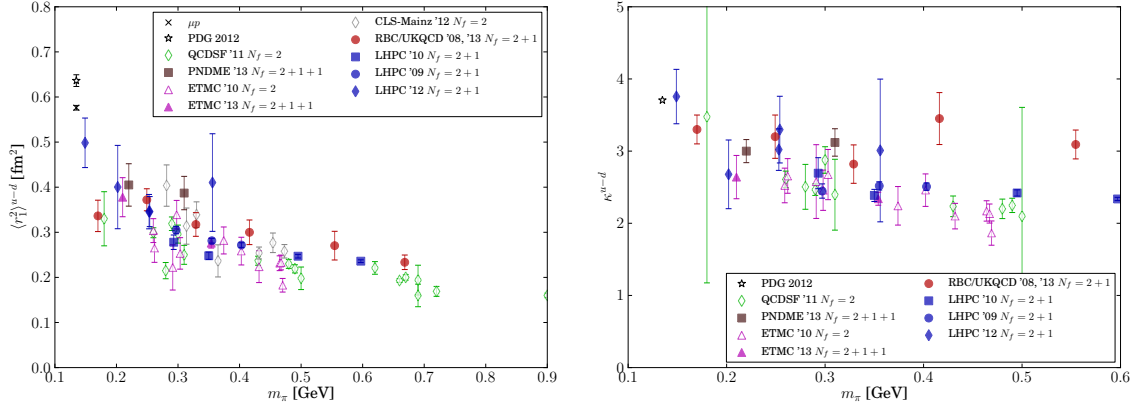


Figure 5: Summary of $(r_1^2)^v$ lattice results [23, 8, 24, 9, 25, 26, 17, 6].

charge and (anomalous) magnetization distributions in the nucleon¹. Calculations of the isovector Dirac radius $(r_1^2)^v$ are tremendously important as a benchmark of lattice QCD, but even more so because of the persisting experimental discrepancy in the proton electric radius (r_{Ep}^2) between measurements involving electrons and muons [29], which might be a signature of new physics phenomena. The two experimental points in Fig. 5 demonstrate this discrepancy in terms of $(r_1^2)^v$, together with a summary of results from different lattice groups. Similarly to $\langle x \rangle_{u-d}$, the isovector radius $(r_1^2)^v$ is also strongly affected by low-energy QCD dynamics, diverging in the chiral limit as $\delta^{\text{ChPT}}(r_1^2)^v \sim \log m_\pi^2$, a likely reason why calculations at heavier pion masses result in values $\approx 50\%$ below experiment. However, many recent lattice QCD calculations with decreasing pion masses do not show a sufficient upward trend. A calculation with $N_f = 2 + 1$ dynamical $\mathcal{O}(a^2)$ -improved Wilson fermions in range $m_\pi \approx 250 \rightarrow 150$ MeV demonstrated that systematic effects from excited states increase dramatically, especially below $m_\pi \lesssim 200$ MeV, and their elimination with the simple “summation” method is sufficient to achieve agreement with experiment [6]. It is also encouraging that the statistical accuracy at the lightest pion mass is comparable to the discrepancy between the two experiments (Fig. 5) and, if improved, may contribute to the resolution of the experimental controversy. It is worth noting that “radii” are usually extracted from form factors using phenomenological fits such as the dipole form. In order to eliminate dependence on fit models, calculations at larger spatial volumes must be performed to have access to smaller values of Q^2 . Finite volume contributions to $G_E(Q^2)$ and (r_E^2) have been computed in effective theory [30] and are sizable, $\delta(r_E^2)^v|_{m_\pi L=4} \approx 0.03(\text{fm})^2$, and thus must be studied as well.

A summary of anomalous magnetic moment $\kappa_v = F_2^{u-d}(0)$ calculations is presented in Fig. 6. This quantity has milder dependence on the pion mass, and its chiral extrapolations and recent calculations close to the physical point are in good agreement with experiment. To compute this quantity, one has to extrapolate the Pauli form factor with $Q^2 \rightarrow 0$; increasing the lattice spatial size L_s will reduce the systematic errors and provide another stringent test of lattice QCD.

¹These quantities should not be literally understood as radii because of relativistic nucleon recoil taking place in measuring these form factors. Note also that experimentalists usually report electric and magnetic Sachs form factors and the corresponding radii $(r_{E,M}^2)$ [28], instead of $(r_{1,2})^2$; these pairs of quantities are linear combinations of each other.

2. Hadron wave functions

Lattice QCD provides a fascinating opportunity to study wave functions of quarks in the nucleon and other hadrons. Although such wave functions have only limited phenomenological meaning and are difficult to compare to experimental data, they can be very illuminating in our understanding of internal structure of hadrons and their excited states. In a calculation very close to the physical point, radial profiles of quark density in the nucleon and its excited states have been studied [31], see Fig. 7. Using a basis of four nucleon interpolating fields composed of quark sources with varied smearing size, the CSSM collaboration has identified, in addition to the nucleon ground state, candidates for $n = 1$ (Roper) and $n = 2$ excitations, which have clearly visible nodes in their radial quark density profile.

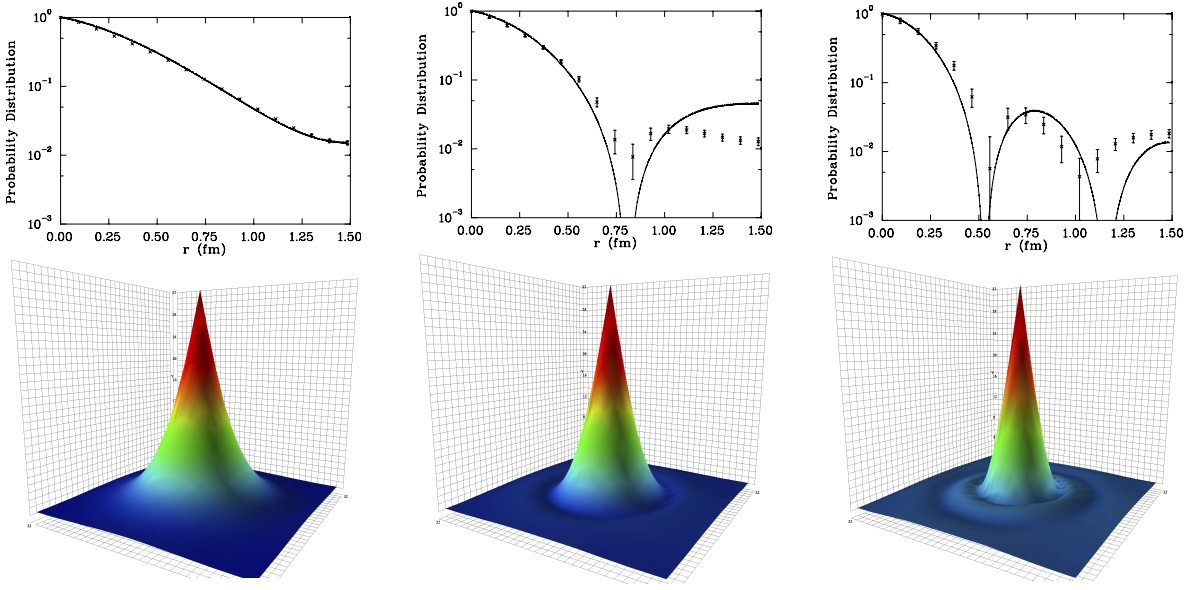


Figure 7: Wave functions of the nucleon and its radial excitations [31].

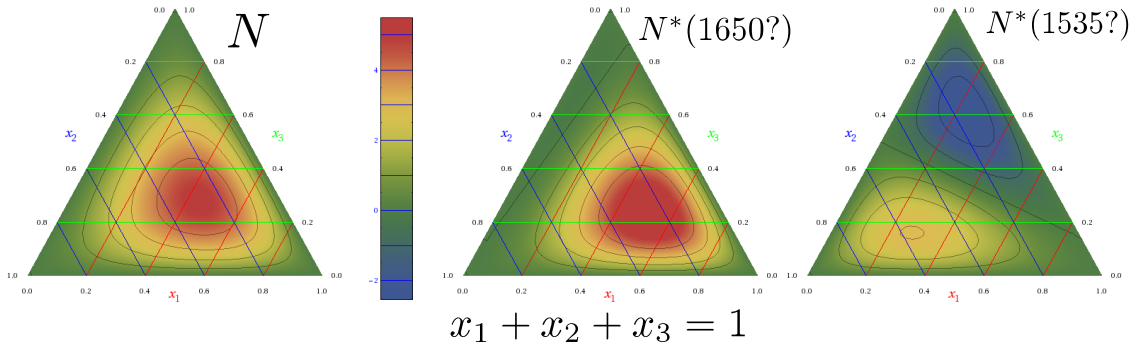


Figure 8: Nucleon distribution amplitudes of valence quarks [32] in coordinates $x_1 + x_2 + x_3 = 1$.

Hadron distribution amplitudes (DA), or partonic wave functions, describe hadron structure in terms of light-cone Fock states. In case of the nucleon, at a sufficiently low scale these wave

functions are dominated by three valence quarks carrying all of the boosted baryon momentum: $x_1 + x_2 + x_3 = 1$, where $x_{1,2,3}$ are valence quark momentum fractions. Distribution amplitudes cannot be computed directly on a lattice because probing a partonic wave function requires an operator with quarks separated along a light-cone direction. Instead, DAs are parameterized as polynomials in $x_{1,2,3}$; the polynomial coefficients are called “shape parameters” and correspond to local operators calculable on a lattice. Figure 8 shows results of a recent lattice calculation [32] where distribution amplitudes of the nucleon and its excited states were computed using $N_f = 2$ dynamical Wilson fermions.

3. Hadron form factors

3.1 Nucleon electromagnetic (vector) form factors

Nucleon Dirac and Pauli form factors $F_{1,2}(Q^2)$ defined in Eq. (1.3) are among the main characteristics of nucleon structure. Interest in the nucleon form factors have been reignited in the recent years when more precise experiments became available in a wide range of momentum Q^2 . These form factors can also be considered benchmark quantities in addition to those discussed in Sec. 1. In addition to verifying the methodology, lattice QCD calculations of the form factors may help resolve some experimental uncertainties. For example, proton form factor measurements are subject to corrections from 2γ exchange, while neutron studies must be conducted on nuclei and therefore have nuclear model uncertainties.

In Figure 9, two recent calculations [10, 8] of nucleon isovector form factors $F_{1,2}^{u-d}(Q^2)$ are compared. Both calculations use $N_f = 2 + 1$ dynamic Wilson fermion action and incorporate advanced methods to isolate the ground state from excited states, which has been demonstrated to have dramatic impact on calculations of the isovector radii [6]. The panels on the right show form factors computed close to the physical point ($m_\pi = 149\text{MeV}$), which agree nicely with the phenomenological fit to experimental data. Calculations with heavier pion masses $m_\pi = 310, 220\text{ MeV}$ shown on the left disagree with the experimental fit, especially form factor F_1 at intermediate momenta $Q^2 \gtrsim 0.5\text{ GeV}^2$. This disagreement driven by heavy pion masses is surprising, since naively one would expect that the low-energy dynamics governed by the pion mass should not influence the structure of the nucleon at momenta $Q^2 \gg m_\pi^2$. There is only little, borderline-significant downward trend in the form factor values between $m_\pi = 310$ and 220 MeV in Fig.9(left), also noticed earlier in the range $m_\pi \approx 300 \dots 400\text{ MeV}$ [26], suggesting that an abrupt change must take place between $m_\pi \approx 200\text{ MeV}$ and the physical point.

3.2 Nucleon axial form factors

Nucleon axial form factors characterize nucleon structure with respect to the density of the axial vector quark current,

$$\langle N(P+q) | \bar{u} \gamma^\mu \gamma^5 u - \bar{d} \gamma^\mu \gamma^5 d | N(P) \rangle = \bar{u}_{P+q} [G_A^q(Q^2) \gamma^\mu \gamma^5 + G_P^q(Q^2) \frac{\gamma^5 q^\mu}{2M_N}] u_P, \quad (3.1)$$

where G_A and G_P are axial and induced pseudoscalar form factors, respectively. Experimental data on these form factors come from measurements of neutrino scattering, charged pion electroproduction and muon capture experiments [35].

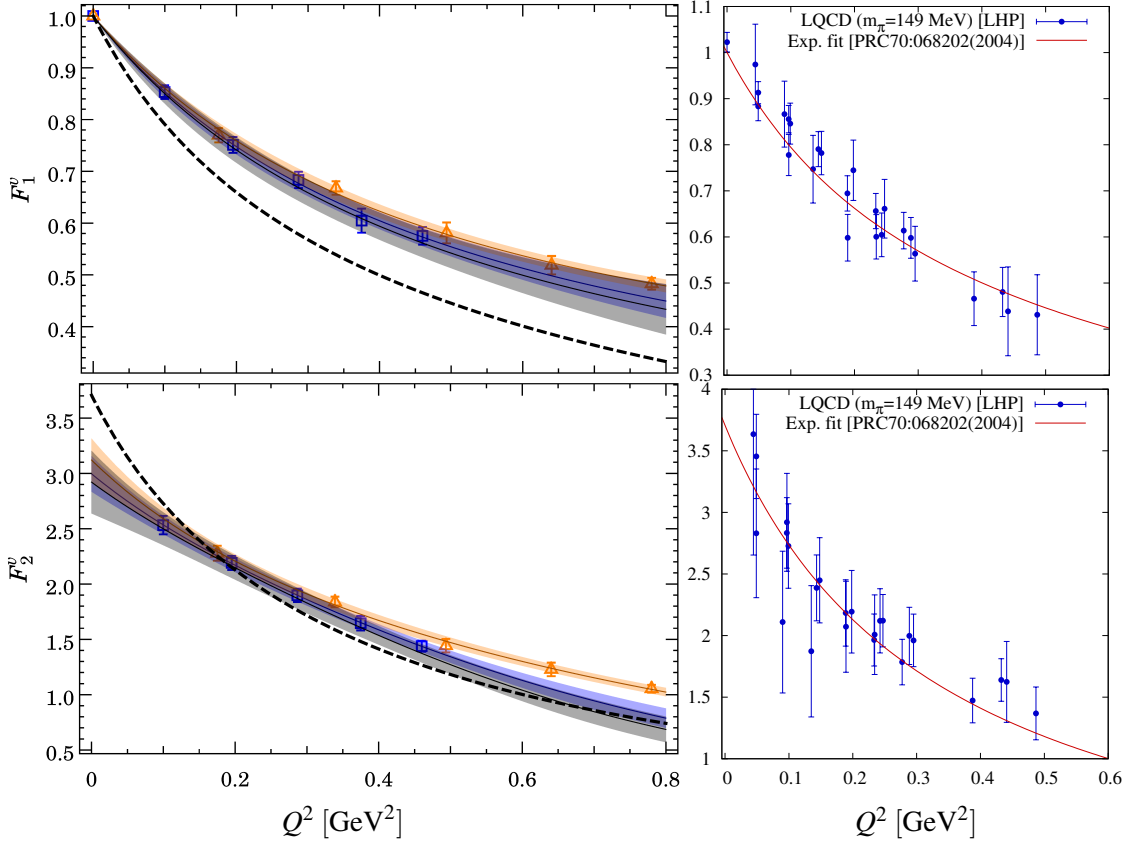


Figure 9: Comparison of the nucleon isovector electromagnetic form factors $F_{1,2}(Q^2)$ computed with $m_\pi = 310, 220$ MeV [8] (left, triangles and squares, respectively) and $m_\pi = 149$ MeV [10] (right). Experimental parameterizations are from Ref. [33] (dashed line, left) and Ref. [34] (solid line, right).

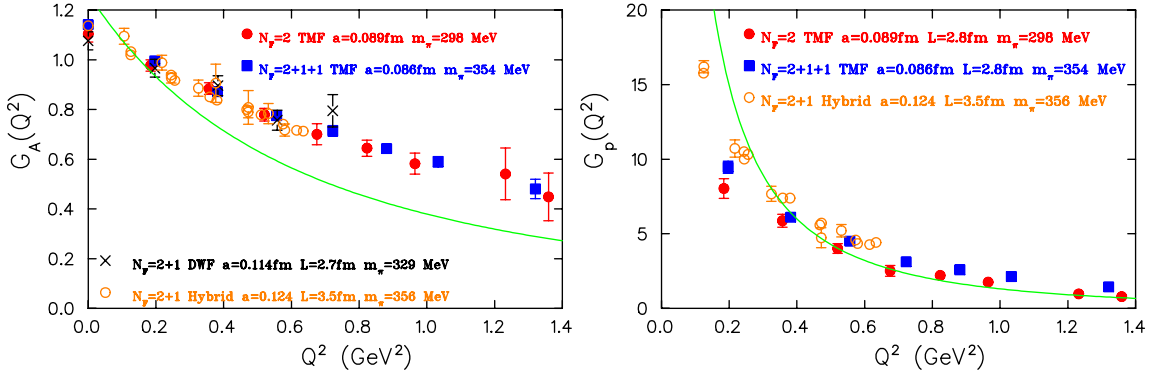


Figure 10: Nucleon axial $G_A(Q^2)$ (left) and induced pseudoscalar $G_P(Q^2)$ form factors [9]. The solid lines are the dipole fit to G_A (left) and the pion pole dominance fit to G_P (right) experimental data (not shown).

Figure 10 displays the summary of lattice data on $G_{A,P}$ form factors calculated with various actions. The left panel shows the axial form factor G_A together with a phenomenological dipole fit to experimental points data (not shown). The axial radius r_A^2 defined similarly to EM radii in Sec. 1.3 as the slope $(-6)(dG_A(Q^2)/dQ^2)|_{Q^2=0}$ is underestimated by $\approx 50\%$ for all pion mass values $m_\pi \geq 213$ MeV, and it shows very little variation with the pion mass in the entire range

$m_\pi = 213 \dots 373$ MeV [9]. This non-trivial effect makes extrapolations based on baryon Chiral Perturbation Theory questionable, since the NLO Lagrangian [36] does not contain any terms to account for m_π dependence, thus requiring higher orders of baryon ChPT at pion masses as small as $m_\pi \approx 200$ MeV.

The induced pseudoscalar form factor G_P is special as it is governed by the intermediate pion pole $\sim (Q^2 + m_\pi^2)^{-1}$ in the coupling of the operator (3.1) to the nucleon. Clearly, this form factor must depend strongly on the pion mass, becoming a steeper function of Q^2 with decreasing m_π . However, the most recent G_P results [9] exhibit very little dependence on m_π ; this may be either a non-trivial low-energy effect similar to the one seen in G_A form factor data, or, as suggested in Ref. [9], may be caused by finite volume effects. This fact makes accurate lattice calculation very challenging, especially in the region of low momenta $Q^2 \sim m_\mu^2$ relevant for phenomenology, where muon capture experiments $\mu + p \rightarrow \nu_\mu + n$ can now measure G_P with substantially improved precision [37].

3.3 Form factors of the pion and Λ

Lattice QCD enables studying properties of hadrons that are not available or very difficult in experiments, such as mesons or unstable baryons containing heavy quarks. For example, computing structure of strange baryons enables testing hypotheses about their internal dynamics. In a recent study [38], electric form factors of Λ and $\Lambda(1405)$ were computed with the help of the variational method (see Fig. 11). From the picture, one can conclude that the mean squared radius of s -quark distribution is enhanced when comparing $\Lambda(1405)$ with Λ , while the radius of light u, d -quarks is shrunk, as m_π goes to the physical point. Such differences support the theory that $\Lambda(1405)$, a $0(\frac{1}{2}^-)$ state, has a significant component of the “molecular” $\bar{K}N$ state, in which the heavier nucleon is surrounded by the cloud of the $\bar{K} = s\bar{q}_{\text{light}}$ meson.

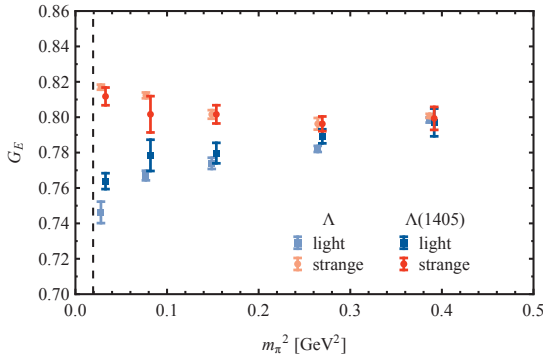


Figure 11: G_E form factor at $Q^2 = 0.16$ GeV² for Λ and $\Lambda(1405)$ [38].

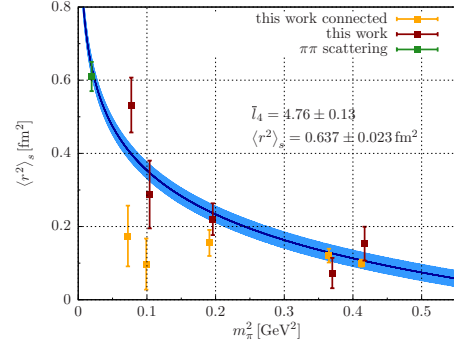


Figure 12: Scalar radius of the pion, full and connected-only terms [39], $N_f = 2$ dynamical fermions.

Another example is the scalar radius of the pion for which only phenomenological estimates exist. A few studies have been performed that disagreed with this estimate by a factor of two. A recent study [39], however, has taken into account disconnected quark contractions, that turned out to be comparable in magnitude to the connected terms, see Fig. 12. The resulting values agree nicely with the NLO prediction of ChPT in a range of pion masses, and the extrapolated value

agrees with phenomenology at the physical pion mass. This agreement confirms the validity of ChPT in the meson sector and provides an additional method to determine low energy constants of the theory, with the ultimate goal to determine all the parameters from first principles.

4. Origin of the proton spin

The proton spin puzzle is the experimental fact that the spins of quarks comprise only $\approx 30 - 50\%$ of the full $\frac{1}{2}$ -spin of the nucleon. The missing part of the nucleon spin can be generated by the orbital motion of quarks and angular momentum of the glue. Size of their contributions can be computed on a lattice with the help of generalized form factor formalism², in which quark and gluon momentum and angular momentum can be defined in a gauge-invariantly [41]:

$$\langle N(P + \frac{1}{2}q) | T_{(\mu\nu)}^{q,g} | N(P - \frac{1}{2}q) \rangle = \bar{u}_{P+\frac{1}{2}q} [A_{20}^{q,g} \gamma_{(\mu} P_{\nu)} + B_{20}^{q,g} \frac{P_{(\mu} i\sigma_{\nu)\rho} q^{\rho}}{2M_N} + C_2^{q,g} \frac{q_{(\mu} q_{\nu)}}{M_N}] u_{P-\frac{1}{2}q} \quad (4.1)$$

where $T_{\mu\nu}^{q,g}$ is the energy-momentum tensor of quarks or gluons and $(\mu\nu)$ above denotes symmetrization over the indices and subtraction of the trace. The generalized form factors $\{A_{20}, B_{20}, C_2\}^{q,g}(Q^2)$ depend on the momentum transfer $Q^2 = -q^2$ and their forward values at $Q^2 \rightarrow 0$ give the size of momentum fraction and angular momentum carried by quarks and gluons,

$$\langle x \rangle_{q,g} = A_{20}^{q,g}(0), \quad J_{q,g} = \frac{1}{2} [A_{20}^{q,g}(0) + B_{20}^{q,g}(0)]. \quad (4.2)$$

In the case of quarks, the angular momentum above is a sum of orbital momentum and spin; for gluons, spin and orbital motion cannot be separated in a gauge-invariant way in this formalism.

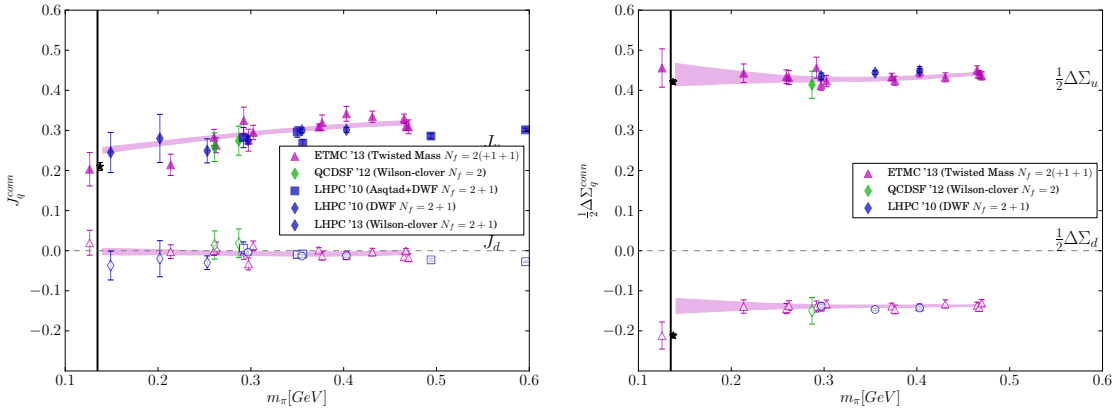


Figure 13: Angular momentum J_q (left) and spin $\frac{1}{2}\Sigma_q$ (right) [9, 42, 17, 43] of light quarks in the proton (connected contributions only) computed with dynamical fermions.

Multiple groups have computed connected contributions to the light quark angular momentum J^q , see Fig. 13(left) for the summary. These quantities apparently have only mild dependence on the pion mass, and there is good agreement across calculations done with a variety of different actions and lattice volumes. Qualitatively, the angular momentum is carried only by the u -quark,

²Recently it has also been suggested that parton distribution functions can be studied directly on a lattice [40].

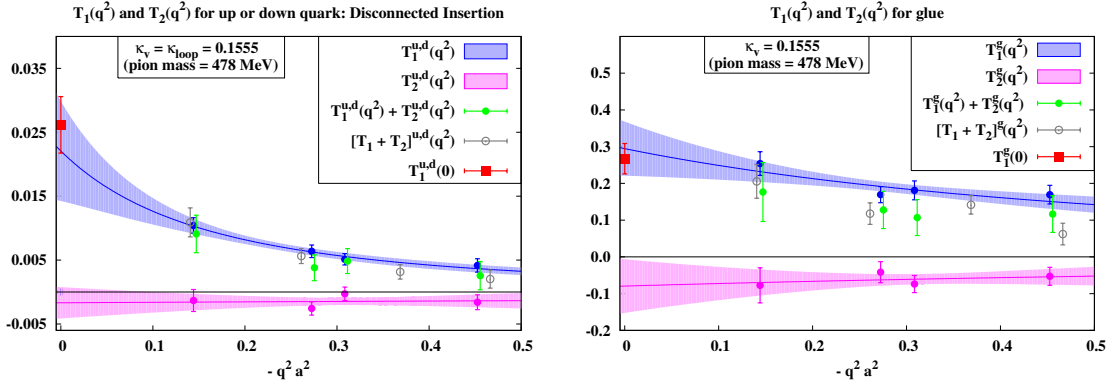


Figure 14: Generalized form factors $T_1 \equiv A_{20}$, $T_2 \equiv B_{20}$ and angular momentum $2J_q = T_1^q(0) + T_2^q(0) \equiv A_{20}^q(0) + B_{20}^q(0)$ of quarks (disconnected contractions) (left) and gluons (right) computed with quenched Wilson fermions [44].

and the d -quark angular momentum is dramatically smaller³. The smallness of J^d , however, is not a trivial fact since the d -quark spin and orbital angular momentum (OAM) appear to cancel each other, at least their connected parts (see Fig. 13, left).

The full calculation of all the contributions to the proton spin [44] has been performed only with quenched fermions and relatively heavy pions $m_\pi \geq 478$ MeV so far. This simplification is justified in order to have a complete picture of separate contributions to the proton spin, the most challenging of which are the quark-disconnected contributions to J^q and the gluon angular momenta J^g , both shown in Fig. 14. The disconnected light-quark angular momentum J_{disc}^{u+d} is small (approximately 7% of the proton spin), while the glue angular momentum was found to comprise $\approx 25\%$ of the proton spin.

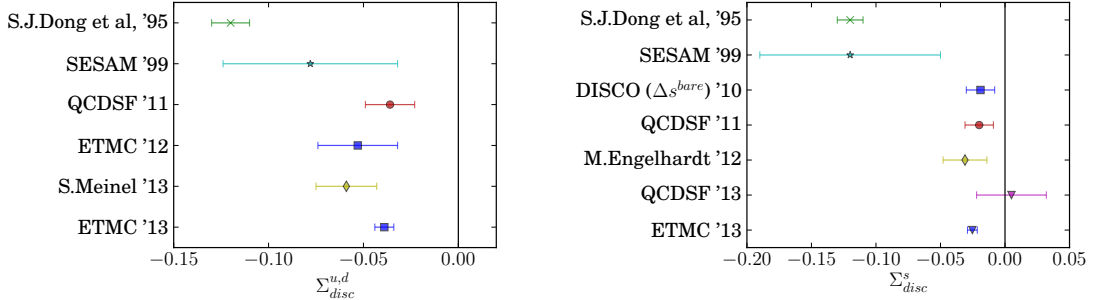


Figure 15: Light quark spin (disconnected contractions) $\Sigma^{u,d}$ [45, 46, 14, 47, 48] (left) and strange quark spin Σ^s [45, 46, 49, 14, 14, 50, 51] (right).

The valence u, d -quark spin $\frac{1}{2}\Sigma_{u,d}$ can be computed on a lattice using the quark spin operator $\bar{q}\gamma_\mu\gamma_5 q$. Note that the spins of individual quarks depend on the hard-to-calculate disconnected contractions; systematic problems in computing $g_A = \Sigma_u - \Sigma_d$ discussed in Sec. 1 may also contribute

³The quark angular momentum is a scale-dependent quantity and the qualitative statements must be made with respect to a certain renormalization scheme and scale. In addition, isoscalar light-quark (angular) momentum mixes with that of the gluon. All results discussed in this review are converted to $\overline{MS}(2 \text{ GeV})$ and mixing with gluons are ignored.

to uncertainties of the individual quark spins. The summary of quark spin lattice data (connected part) is presented in Fig. 13(right), which exhibits little dependence on the pion mass and also decent agreement between different lattice methodologies and phenomenology.

Disconnected contributions to the light quark spin were computed for the first time in Ref. [45], and were found to be quite large. A series of new calculations performed in recent years found smaller values for $\Sigma_{u,d}^{\text{disc}}$, as shown in Fig. 15(left); the discrepancy is likely due to the quenched action used in Ref. [45]. For the strange quark, the newer, unquenched calculations also result in much smaller values for the strange quark spin compared with quenched one [45], see Fig. 15(right). Whether disconnected contributions are large or small may change our view on the role of the quark orbital angular momentum (OAM) in the proton⁴ dramatically: if only the connected contributions are taken into account (or the disconnected contributions are small), the $u + d$ quark OAM is very small [17, 42, 9]; however, if the disconnected contributions are large, then the quark OAM may be responsible for almost half of the proton spin [44].

5. Conclusions

At the present moment, many hadron structure calculations are already performed at the physical point. This fascinating achievement makes lattice QCD much more robust at once, since chiral extrapolations are no longer needed, thus eliminating the largest source of systematic uncertainty.

However, the first results indicate strongly that other systematic problems specific to hadron structure calculations are more severe in comparison with studies with heavier pions. For example, the isovector Dirac radius of the nucleon is affected by substantial contributions from excited states, and so is the isovector quark momentum fraction. This fact makes careful assessment of excited states and other systematic effects the top priority, especially for the “benchmark quantities” that are used to validate lattice QCD methodology. In particular, the nucleon radii can already be computed with statistical uncertainty that is comparable to the currently observed discrepancy in the determination of the proton electric radius; the systematic uncertainties, however, may preclude meaningful comparison to the experiment.

Other systematic uncertainties such as finite volume and discretization errors are, in general, small compared with the excited state contributions. This may change in the nearest future with accumulation of statistics in the on-going calculations and addition of lattice calculations with larger volumes and lattice spacings. Calculations with larger volumes and smaller lattice spacings are also extremely important for studies of hadron form factors, where wider kinematic regions are relevant for phenomenology and comparisons to the experiment. Larger lattice spatial volumes help study form factors close to the forward limit ($Q^2 = 0$), determine “radii” and extract couplings such as g_p . Smaller lattice spacings are important for the proton form factors G_{Ep} and G_{Mp} in the large momentum region $Q^2 \gtrsim 1 \text{ GeV}^2$, where new experimental data disagree with previous studies and reshape our understanding of the proton structure.

Complete calculation of contributions to the proton spin has only been performed with quenched lattices. In that study, u, d, s quark spins from disconnected contractions are large, leading to the

⁴The quark OAM in this context has only naive meaning as the difference $L_q = J_q - \frac{1}{2}\Sigma_q$; however, the proximity of both L_{u+d} and the nucleon anomalous magnetic moment κ^{u+d} to zero may be a hint that this definition is an important phenomenological quantity.

conclusion that substantial fraction of the proton spin comes from the quark orbital angular momentum. Some initial calculations with fully dynamical quarks indicate that these disconnected contributions are substantially smaller, leading to smaller quark OAM. However, a complete calculation of all the components is required in order to make a definite conclusion.

References

- [1] S. Durr et al., *Ab-Initio Determination of Light Hadron Masses*, *Science* **322** (2008) 1224–1227, [[arXiv:0906.3599](#)].
- [2] **RBC+UKQCD Collaboration** Collaboration, T. Yamazaki et al., *Nucleon axial charge in 2+1 flavor dynamical lattice QCD with domain wall fermions*, *Phys.Rev.Lett.* **100** (2008) 171602, [[arXiv:0801.4016](#)].
- [3] B. J. Owen, J. Dragos, W. Kamleh, D. B. Leinweber, M. S. Mahbub, et al., *Variational Approach to the Calculation of g_A* , *Phys.Lett.* **B723** (2013) 217–223, [[arXiv:1212.4668](#)].
- [4] S. Capitani, M. Della Morte, G. von Hippel, B. Jager, A. Juttner, et al., *The nucleon axial charge from lattice QCD with controlled errors*, *Phys.Rev.* **D86** (2012) 074502, [[arXiv:1205.0180](#)].
- [5] B. Jäger, T. Rae, S. Capitani, M. Della Morte, D. Djukanovic, et al., *A high-statistics study of the nucleon EM form factors, axial charge and quark momentum fraction*, [arXiv:1311.5804](#).
- [6] J. Green, M. Engelhardt, S. Krieg, J. Negele, A. Pochinsky, et al., *Nucleon Structure from Lattice QCD Using a Nearly Physical Pion Mass*, [arXiv:1209.1687](#).
- [7] S. Dinter, C. Alexandrou, M. Constantinou, V. Drach, K. Jansen, et al., *Precision Study of Excited State Effects in Nucleon Matrix Elements*, *Phys.Lett.* **B704** (2011) 89–93, [[arXiv:1108.1076](#)].
- [8] T. Bhattacharya, S. D. Cohen, R. Gupta, A. Joseph, and H.-W. Lin, *Nucleon Charges and Electromagnetic Form Factors from 2+1+1-Flavor Lattice QCD*, [arXiv:1306.5435](#).
- [9] C. Alexandrou, M. Constantinou, S. Dinter, V. Drach, K. Jansen, et al., *Nucleon form factors and moments of generalized parton distributions using $N_f = 2 + 1 + 1$ twisted mass fermions*, *Phys.Rev.* **D88** (2013) 014509, [[arXiv:1303.5979](#)].
- [10] J. Green, M. Engelhardt, S. Krieg, S. Meinel, J. Negele, et al., *Nucleon form factors with light Wilson quarks*, [arXiv:1310.7043](#).
- [11] C. Alexandrou, M. Constantinou, V. Drach, K. Jansen, C. Kallidonis, et al., *Nucleon generalized form factors with twisted mass fermions*, [arXiv:1312.2874](#).
- [12] **ETM Collaboration**, C. Alexandrou et al., *Axial Nucleon form factors from lattice QCD*, *Phys.Rev.* **D83** (2011) 045010, [[arXiv:1012.0857](#)].
- [13] C. Alexandrou, M. Constantinou, S. Dinter, V. Drach, K. Jansen, et al., *Excited State Effects in Nucleon Matrix Element Calculations*, *PoS LATTICE2011* (2011) 150, [[arXiv:1112.2931](#)].
- [14] **QCDSF Collaboration**, G. S. Bali et al., *Strangeness Contribution to the Proton Spin from Lattice QCD*, *Phys.Rev.Lett.* **108** (2012) 222001, [[arXiv:1112.3354](#)].
- [15] R. Horsley, Y. Nakamura, A. Nobile, P. Rakow, G. Schierholz, et al., *Nucleon axial charge and pion decay constant from two-flavor lattice QCD*, [arXiv:1302.2233](#).
- [16] **RBC / UKQCD Collaboration**, S. Ohta, *Nucleon axial charge in 2+1-flavor dynamical DWF lattice QCD*, [arXiv:1309.7942](#).

- [17] **LHP** Collaboration, J. Bratt et al., *Nucleon structure from mixed action calculations using 2+1 flavors of asqtad sea and domain wall valence fermions*, *Phys.Rev.* **D82** (2010) 094502, [[arXiv:1001.3620](#)].
- [18] Y. Aoki, T. Blum, H.-W. Lin, S. Ohta, S. Sasaki, et al., *Nucleon isovector structure functions in (2+1)-flavor QCD with domain wall fermions*, *Phys.Rev.* **D82** (2010) 014501, [[arXiv:1003.3387](#)].
- [19] G. S. Bali, S. Collins, M. Deka, B. Glassle, M. Gockeler, et al., $\langle x \rangle_{u-d}$ from lattice QCD at nearly physical quark masses, *Phys.Rev.* **D86** (2012) 054504, [[arXiv:1207.1110](#)].
- [20] **QCDSF/UKQCD** Collaboration, D. Pleiter et al., *Nucleon form factors and structure functions from $N(f)=2$ Clover fermions*, *PoS LATTICE2010* (2010) 153, [[arXiv:1101.2326](#)].
- [21] G. Martinelli, C. Pittori, C. T. Sachrajda, M. Testa, and A. Vladikas, *A General method for nonperturbative renormalization of lattice operators*, *Nucl. Phys.* **B445** (1995) 81–108, [[hep-lat/9411010](#)].
- [22] G. Bali, S. Collins, B. Gläsel, M. Göckeler, J. Najjar, et al., *Moments of structure functions for $N_f = 2$ near the physical point*, [arXiv:1311.7041](#).
- [23] S. Collins, M. Gockeler, P. Hagler, R. Horsley, Y. Nakamura, et al., *Dirac and Pauli form factors from lattice QCD*, *Phys.Rev.* **D84** (2011) 074507, [[arXiv:1106.3580](#)].
- [24] S. Capitani, M. Della Morte, G. von Hippel, B. Jager, B. Knippschild, et al., *Excited state systematics in extracting nucleon electromagnetic form factors*, *PoS LATTICE2012* (2012) 177, [[arXiv:1211.1282](#)].
- [25] **RBC / UKQCD** Collaboration, M. Lin, *Status of nucleon structure calculations with 2+1 flavors of domain wall fermions*, *PoS LATTICE2012* (2012) 172, [[arXiv:1303.0022](#)].
- [26] S. Syritsyn, J. Bratt, M. Lin, H. Meyer, J. Negele, et al., *Nucleon Structure with Domain Wall Fermions at $a = 0.084$ fm*, *PoS LATTICE2008* (2008) 169, [[arXiv:0903.3063](#)].
- [27] T. Yamazaki et al., *Nucleon form factors with 2+1 flavor dynamical domain-wall fermions*, *Phys. Rev.* **D79** (2009) 114505, [[arXiv:0904.2039](#)].
- [28] **Particle Data Group** Collaboration, J. Beringer et al., *Review of Particle Physics (RPP)*, *Phys.Rev.* **D86** (2012) 010001.
- [29] R. Pohl et al., *The size of the proton*, *Nature* **466** (2010) 213–216.
- [30] J. Hall, D. Leinweber, B. Owen, and R. Young, *Finite-volume corrections to charge radii*, *Phys.Lett.* **B725** (2013) 101–105, [[arXiv:1210.6124](#)].
- [31] D. S. Roberts, W. Kamleh, and D. B. Leinweber, *Wave Function of the Roper from Lattice QCD*, [arXiv:1304.0325](#).
- [32] R. Schiel, *Wave functions of the nucleon and the N^** , in *LATTICE 2013*, 2013.
- [33] J. Arrington, W. Melnitchouk, and J. Tjon, *Global analysis of proton elastic form factor data with two-photon exchange corrections*, *Phys.Rev.* **C76** (2007) 035205, [[arXiv:0707.1861](#)].
- [34] J. J. Kelly, *Simple parametrization of nucleon form factors*, *Phys. Rev.* **C70** (2004) 068202.
- [35] V. Bernard, L. Elouadrhiri, and U. Meissner, *Axial structure of the nucleon: Topical Review*, *J.Phys.* **G28** (2002) R1–R35, [[hep-ph/0107088](#)].

- [36] V. Bernard, H. W. Fearing, T. R. Hemmert, and U. G. Meissner, *The form factors of the nucleon at small momentum transfer*, *Nucl. Phys.* **A635** (1998) 121–145, [[hep-ph/9801297](#)].
- [37] **MuCap** Collaboration, V. Andreev et al., *Measurement of Muon Capture on the Proton to 1% Precision and Determination of the Pseudoscalar Coupling g_P* , *Phys.Rev.Lett.* **110** (2013) 012504, [[arXiv:1210.6545](#)].
- [38] B. J. Menadue, W. Kamleh, D. B. Leinweber, M. S. Mahbub, and B. J. Owen, *Electromagnetic Form Factors for the $\Lambda(1405)$* , [arXiv:1311.5026](#).
- [39] V. Gülpers, G. von Hippel, and H. Wittig, *The scalar pion form factor in two-flavor lattice QCD*, [arXiv:1309.2104](#).
- [40] X. Ji, *Parton Physics on Euclidean Lattice*, *Phys.Rev.Lett.* **110** (2013) 262002, [[arXiv:1305.1539](#)].
- [41] X.-D. Ji, *Gauge invariant decomposition of nucleon spin*, *Phys. Rev. Lett.* **78** (1997) 610–613, [[hep-ph/9603249](#)].
- [42] A. Sternbeck, M. Gockeler, P. Hagler, R. Horsley, Y. Nakamura, et al., *First moments of the nucleon generalized parton distributions from lattice QCD*, *PoS LATTICE2011* (2011) 177, [[arXiv:1203.6579](#)].
- [43] S. Syritsyn, J. Green, J. Negele, A. Pochinsky, M. Engelhardt, et al., *Quark Contributions to Nucleon Momentum and Spin from Domain Wall fermion calculations*, *PoS LATTICE2011* (2011) 178, [[arXiv:1111.0718](#)].
- [44] M. Deka, T. Doi, Y. Yang, B. Chakraborty, S. Dong, et al., *A Lattice Study of Quark and Glue Momenta and Angular Momenta in the Nucleon*, [arXiv:1312.4816](#).
- [45] S. Dong, J.-F. Lagae, and K. Liu, *Flavor singlet $g(A)$ from lattice QCD*, *Phys.Rev.Lett.* **75** (1995) 2096–2099, [[hep-ph/9502334](#)].
- [46] **TXL** Collaboration, S. Gusken et al., *The flavor singlet axial coupling of the proton with dynamical Wilson fermions*, [hep-lat/9901009](#).
- [47] C. Alexandrou, V. Drach, K. Hadjiyiannakou, K. Jansen, G. Koutsou, et al., *Evaluation of disconnected contributions using GPUs*, *PoS LATTICE2012* (2012) 184, [[arXiv:1211.0126](#)].
- [48] A. Abdel-Rehim, C. Alexandrou, M. Constantinou, V. Drach, K. Hadjiyiannakou, et al., *Disconnected quark loop contributions to nucleon observables in lattice QCD*, *Phys.Rev.* **D89** (2014) 034501, [[arXiv:1310.6339](#)].
- [49] R. Babich, R. C. Brower, M. A. Clark, G. T. Fleming, J. C. Osborn, et al., *Exploring strange nucleon form factors on the lattice*, *Phys.Rev.* **D85** (2012) 054510, [[arXiv:1012.0562](#)].
- [50] M. Engelhardt, *Strange quark contributions to nucleon mass and spin from lattice QCD*, *Phys.Rev.* **D86** (2012) 114510, [[arXiv:1210.0025](#)].
- [51] C. Alexandrou, V. Drach, K. Jansen, G. Koutsou, and A. Vaquero, *Computation of disconnected contributions to nucleon observables*, [arXiv:1401.6749](#).